Int. J. Electrochem. Sci., 14 **(2019)** 1283 – 1292, doi: 10.20964/2019.02.43

International Journal of ELECTROCHEMICAL SCIENCE
www.electrochemsci.org

Short Communication

Detection of Residual Methomyl in Vegetables with an Electrochemical Sensor based on a glassy carbon electrode modified with Fe_3O_4/Ag composite

Ke Gai[1,2], *Huili Qi*[2], *Li Xiao li*[2], *Xuefen Liu*[1,*]

[1] College of Energy Engineering, Longdong University, Qingyang, 745000，China.
[2] College Chemistry & Chemical Engineering, Long Dong University, Qing yang, 745000, China.
[*]E-mail: xuefen580@126.com

Received: 10 October 2018 / *Accepted:* 29 November 2018 / *Published:* 5 January 2019

A magnetic Fe_3O_4/Ag composite with a core-shell structure was synthesized using a combination of Fe_3O_4 nanoparticle coprecipitation and the reduction of Ag^+ on the surface of the Fe_3O_4 nanoparticles by trisodium citrate. The as prepared Fe_3O_4/Ag composites was characterized by ultraviolet-visible absorption spectroscopy, and scanning/transmission electron microscopy (SEM and TEM). An electrochemical sensor was prepared by attaching the Fe_3O_4/Ag composites to the surface of a glassy carbon electrode (GCE) using chitosan (CS) as linking molecules. The concentration of methomyl in vegetables was measured using cyclic voltammetry (CV). The linear relationship was achieved in the concentration range of 3.47×10^{-5}～3.47×10^{-4} mol·L^{-1}, with a correlation coefficient R^2 of 0.99707 and a detection limit of 2.97×10^{-5} mol·L^{-1}.

Keywords: Fe_3O_4 Magnetic Nanoparticles; Fe_3O_4/Ag composites; Electrochemical Sensor; Methomyl; Residual Quantity.

1. INTRODUCTION

Methomyl, also known under the trade name Lannate, is a systemic carbamate pesticide with the chemical name S-methyl-N [(methyl carbamoyl)-O] thioacetamide. Methomyl is generally believed to lead to effects such as stomach poisoning, contact killing, and suffocation. Through strong osmotic force, methomyl kills the eggs of pests that are resistant to organo-phosphorus and pyrethroid. Methomyl has been used to prevent and control Lepidoptera, Homoptera, Coleoptera and other mite pests on cotton, vegetables and tobacco. Methomyl can act on the cholinesterase of pests and destroy their nervous systems, eventually killing them. The existing pesticide formulations of methomyl include miscible oil, water aqua, dosage and water-soluble powder. It usually decomposes rapidly on crops and in the environment leaving very small amounts of residue. However, along the food chain, pesticide residue

could be accumulated in more advanced organisms, and consequently threaten human health.

The reported methods to detect methomyl primarily include biosensors, high-performance liquid chromatography-mass spectrometry, fluorescence, liquid chromatography-tandem mass spectrometry, gas chromatography-mass spectrometry, high-performance liquid chromatography, and capillary micellar electrokinetic chromatography [1-7]. Although with low detection limit, relatively accurate results, the aforementioned methods suffer from the disadvantages such as high experimental cost, complicated procedures, rigor experimental conditions, and other inconvenience.

Fe_3O_4 nanoparticles are among the most common magnetic nanoparticles and are widely used in microwave-absorbing materials, information storage, magnetic liquids, medicine, and biomedicine. Due to large specific surface areas, Fe_3O_4 nanoparticles are, however, prone to oxidation and aggregation, which lead to low magnetism and poor dispersion. In recent years, efforts have been made apply certain facial modification on Fe_3O_4 by mean of development of a wide range of composite nanoparticles.

In the present work, a layer of Ag nanoparticles were coated on the surface of Fe_3O_4 magnetic nanoparticles to form Fe_3O_4/Ag composites with core-shell structures. The Fe_3O_4/Ag magnetic composites were then assembled on the surface of the glassy carbon electrode (GCE) using chitosan (CS) as the linking molecules to form a Fe_3O_4/Ag-CS-GCE electrochemical sensor for the detection of methomyl. It is reasonable in cost and easy to operate. The detection method for methomyl developed in the present work exhibits the advantage of strong anti-interference capabilities and high accuracy.

2. EXPERIMENTAL SECTION

2.1. Materials

Methomyl (20%, emulsifiable), dichlorvos (77.5%, emulsifiable), chlorpyrifos (40%, emulsifiable), phoxim (18.5%, emulsifiable), sodium dodecylbenzenesulfonic acid (SDBS), silver nitrate, soluble starch, glucose, potassium ferricyanide (Xi'an Research Reagent Factory), potassium nitrate, chitosan (deacetylation degree 95%), sodium hydroxide, iron sulfate, ferrous sulfate, sulfuric acid, trisodium citrate, sodium dihydrogen phosphate, and disodium hydrogen phosphate were used. The reagents used were analytically pure except soluble starch. Ultra-pure water was used.

2.2. Preparation of Fe_3O_4 nanoparticles and Fe_3O_4/Ag composites

The preparation of Fe_3O_4/Ag magnetic nanomaterial consists of two parts [8].

First, 120 mL of 1.5 mol·L^{-1} NaOH aqueous solution was put into a flask and then heated to 80℃. Second, 4.30 g $Fe_2(SO_4)_3 \cdot XH_2O$, 1.50 g $Fe_2SO_4 \cdot 7H_2O$ and 2 mL of 2 mol·L^{-1} H_2SO_4 was put into and thoroughly mixed with 20 mL of ultra-pure water. The mixture was gradually dripped into the NaOH solution at 80 °C in the four-neck flask and allowed to react for 1 h. Finally, magnetic Fe_3O_4 nanoparticles were obtained through magnetic field separation.

In the second part, 145 mL of 11.0×10 mol·L^{-1} trisodium citrate aqueous solution, 1 mL of 0.7 mol·L^{-1} sodium dodecylbenzenesulfonic acid solution and 0.15 g of the as-prepared magnetic Fe_3O_4 nanoparticles were put into a round-bottom flask. The mixture was then heated to boiling and kept

boiling while 50 mL of 4×10 mol·L^{-1} silver nitrate aqueous solution was quickly dropwise added into the flask; the final mixture was left to react for 30 minutes. Finally, the magnetic Fe_3O_4/Ag composite product was obtained by filtration-drying and magnetic separation. It was set aside.

2.3. Preparation of nano Ag

We put 0.1 g of soluble starch and 2~3 drops of 0.05 mol·L^{-1} silver nitrate solution into 25 mL of distilled water in a beaker. After adding 0.02 g dihydrate of trisodium citrate and 0.03 g glucose, the mixture was heated for 9 minutes in a household microwave. Finally, the nano Ag buffer solution was successfully prepared [9].

2.4. Modification of electrode and preparation of electrochemical sensor

The bare glassy carbon electrode (GCE) was polished to a mirror finish with 0.3 μm and 0.05 μm Al_2O_3 paste and treated by ultrasound in acetone (1 mol·L^{-1}) and secondary water [10]. Before the modification, the glassy carbon electrode was placed in a mixture of potassium ferricyanide and potassium nitrate at defined concentrations and scanned in the potential range from -0.2 V to 0.6 V to get a stable cyclic voltammogram. The pretreated GCE was placed in a defined amount of dispersed solution of Fe_3O_4/Ag nanoparticles. We premixed 0.02 g chitosan (CS) with 1 mL of acetic acid solution evenly. An aliquot of 5 μL of such a mixture was dispensed on the GCE surface modified with nanoparticles, and the treated electrode was left in the air to dry. Finally, a Fe_3O_4/Ag-CS-GCE chemical sensor was obtained [11-12]. This paper adopted a three-electrode system, with saturated calomel electrode (SCE) as the reference electrode, platinum wire electrode as the counter-electrode, and GCE as the working electrode.

2.5. Characterization

The morphology of the as-prepared nanocomposite was examined with a scanning electron microscope (SEM, JEOL JSM-6510LV) and by transmission electron microscopy (TEM, FEI Tecnai G20). To understand the morphology and internal structure of the samples, the morphology of the Fe_3O_4/Ag composites was examined by SEM and TEM at different magnifications [13]. The UV-vis diffuse reflectance spectra of the samples were obtained for the dry-pressed film samples using a UV-vis spectrophotometer (SPECORD50 PLUS, Analytik Jena). $BaSO_4$ was used as a reflectance standard in the UV-vis diffuse reflectance experiment. In addition, the test instruments included an electronic balance (BS110S); quartz UV cuvette; KQ3200 ultrasonic processing equipment; PHS-3C Rex pH meter; PJ25B-A microwave oven; beaker (50 mL, 100 mL); RST electrochemical workstation (Zhengzhou Cirusi instrument technology Co., LTD.); and electric stove.

3. RESULTS AND DISCUSSION

3.1. Structures and morphology

Fig. 1a shows that when the sample was enlarged by 70,000 times, it appeared as an agglomerated form. One kind of agglomerate is shown in Fig 1b, with different shapes and an average size of ~2 μm in diameter. Further amplification was able to resolve the roughness of the surface of this single agglomerate (shown in Fig. 1c). Fig. 1d, Fig. 1e and Fig. 1f are the TEM images of Fe_3O_4 and Fe_3O_4/Ag nanoparticles. Fig. 1d indicates that the particle size of Fe_3O_4 nanoparticles was approximately 2~5 nm, with a spherical morphology. Upon modification by the Ag shell, the particle size changed to 20~50 nm, indicating that a group of Fe_3O_4 particles was parceled by Ag nanoparticles. The core-shell structure is clearly exhibited in Fig. 1f, with a shell thickness of a few nm.

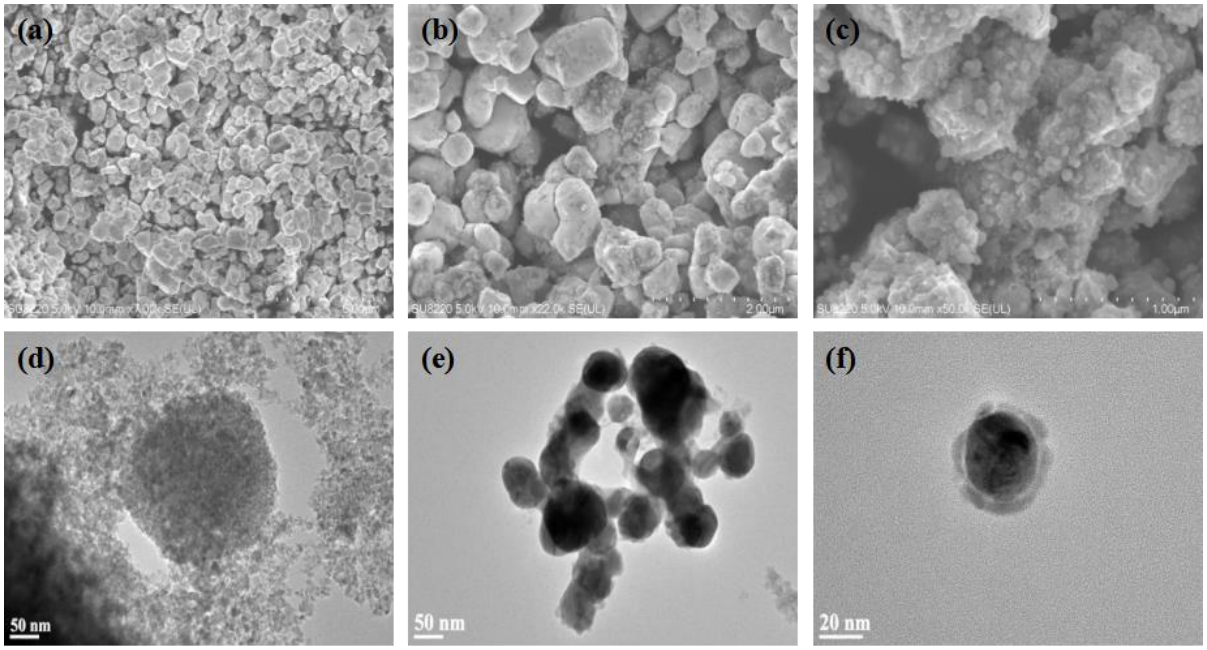

Figure 1. (a) (b) (c) SEM images of Fe_3O_4/Ag composites, (d) TEM image of Fe_3O_4 nanoparticles, (e) (f) TEM images of Fe_3O_4/Ag composites

3.2. UV-vis diffuse reflectance spectroscopy

To further identify whether the Fe_3O_4 nanoparticles were successfully coated with Ag or Ag nanoparticles, UV-vis diffuse reflectance spectra (DRS) of Ag, Fe_3O_4 and Fe_3O_4/Ag composites were collected. As shown in Fig. 2, the Fe_3O_4 nanoparticles had no obvious absorption peak in the ultraviolet-visible region. Ag nanoparticles and Fe_3O_4/Ag composites presented absorption peaks at 411 nm and 415 nm, respectively. The peak position of Fe_3O_4/Ag composites was shifted to a longer wavelength than that of Ag nanoparticles, while the peak shape became wider and weaker due to the contribution of the rather dark center of Fe_3O_4[13].

Because the particle size of Fe_3O_4/Ag was relatively small and evenly distributed as a spherical morphology, these particles can be modeled as a uniform electric field with phase, showing a simple dipole resonance mode. When incident light was irradiated through the nanoparticles in aqueous solution, it generated a large and waning characteristic absorption peak. The peak shift is likely caused by the resonance absorption of this composite system and the superposition of nano-Fe_3O_4 background and nano Ag [8]. After all, the UV-vis diffuse spectroscopy indicates that Ag nanoparticles were successfully coated on the surface of Fe_3O_4 particles; however, the coating is not evenly over the entire surface. This is consistent with the TEM results.

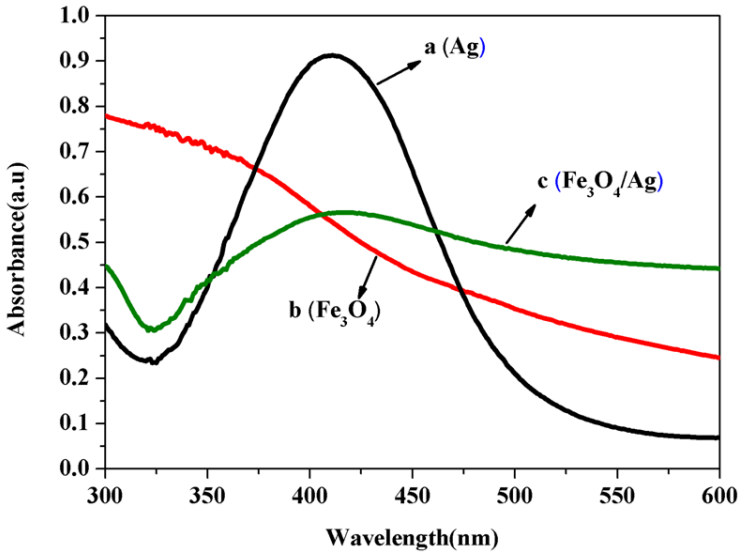

Figure 2. UV-vis of nanoparticles: (a) Ag nanoparticles (b) Fe_3O_4 nanoparticles (c) Fe_3O_4/Ag composites

3.3. Optimization of conditions

The supporting electrolyte is a very important parameter in electroanalytical method[14]. The voltammograms of methomyl (1.04×10^{-4} mol·L^{-1}) with an electrode modified by Fe_3O_4/Ag nanoparticle were compared in different supporting electrolytes (pH =7.0). The best results for the current response and peak shape of methomyl were obtained in 0.2 M phosphate buffer solution. Therefore, the following tests were performed in 0.2 M phosphate buffer.

To study the impact of the pH , the current response of methomyl was measured at the pH values of 6.80, 6.85, 6.90, 6.95 and 7.00, while fixing the concentration of methomyl at 1.04×10^{-4} mol·L^{-1}. The value of the current response shown in Fig. 3 first increases then decreases with the increase of pH in the range of 6.8 ~ 7.0. The maximum current response was reached at pH 6.9.

The dosage of the Fe_3O_4/Ag composites solution was optimized by applying 5 μL, 7 μL, 10 μL, 12 μL, and 15 μL respectively. As the dosage of the Fe_3O_4/Ag composites solution increases, the current response of methomyl first increases and then decreases, as shown in Fig. 4. The maximum current response was achieved at the dosage of 10 μL.

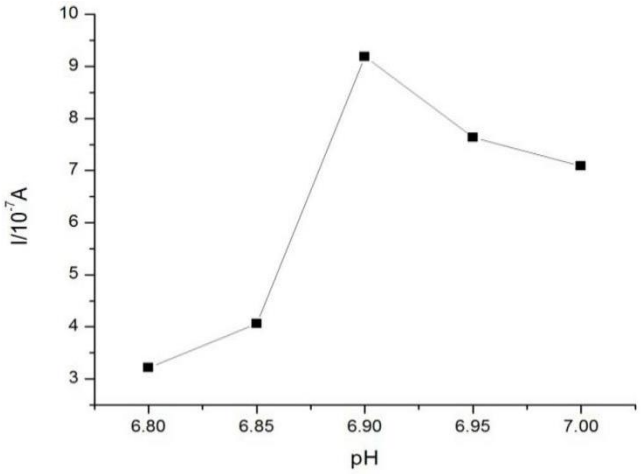

Figure 3. Impact of pH on the current response of the sensor ($C_{Met\,hom\,yl}$=1.04×10^{-4} mol·L^{-1},$V_{Fe_3O_4/Ag}$ =10μL,T=298 K)

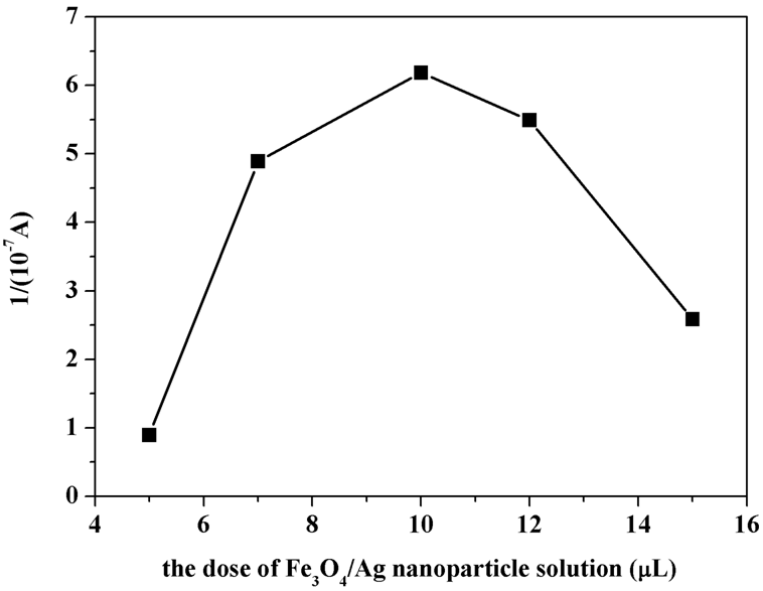

Figure 4. Relationship between the dose of Fe_3O_4/Ag nano-solution and current intensity ($C_{Met\,hom\,yl}$ =1.04×10^{-4} mol·L^{-1}, $V_{Fe_3O_4/Ag}$ =10μL, pH=6.9, T=298 K)

The cyclic voltammogram scan was performed at different rates using the modified electrode by Fe_3O_4/Ag nanoposites in methomyl at the concentration of 1.04×10^{-4} mol·L^{-1}. The results in Fig. 5 indicate while the current intensity increases with an increase in scan rate, and the reduction peak current is found proportional to the square root of scan rate, a typical correlation for a diffusion-controlled process[15]. The linear relationship between the reduction peak current and the square root of the scan rate is observed in the rate range of 0.025～0.1 V·s^{-1}. However, if the scan rate is set too high, the background current becomes more obvious and interferes with the measurement. In the present work, the scanning rate was set at 0.05 V·s^{-1} to obtain the optimal signal-to-noise ratio.

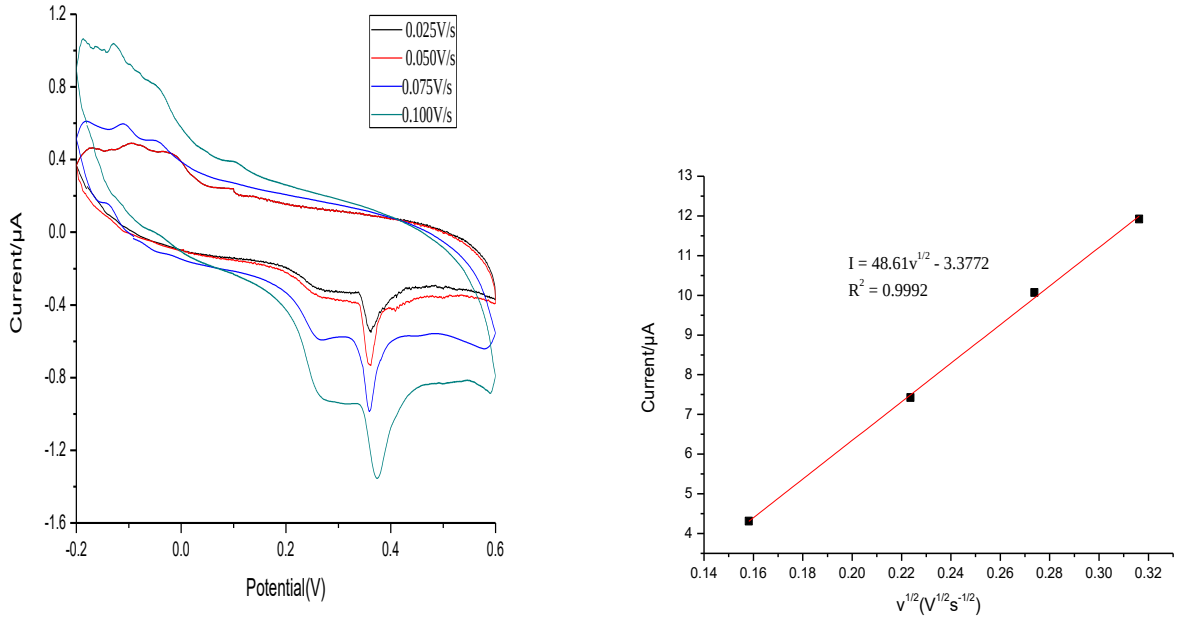

(a) (b)

Figure 5. (a) Cyclic voltammogram of Fe_3O_4/Ag-GCE in methomyl solution with different scan rates. (b) Current intensity of Fe_3O_4/Ag-GCE in methomyl with different scan rates. ($C_{Met\,hom\,yl}$ =1.04× 10^{-4} mol·L^{-1}, $V_{Fe_3O_4/Ag}$ =10μL, pH=6.9, T=298 K)

3.4 The standard curve

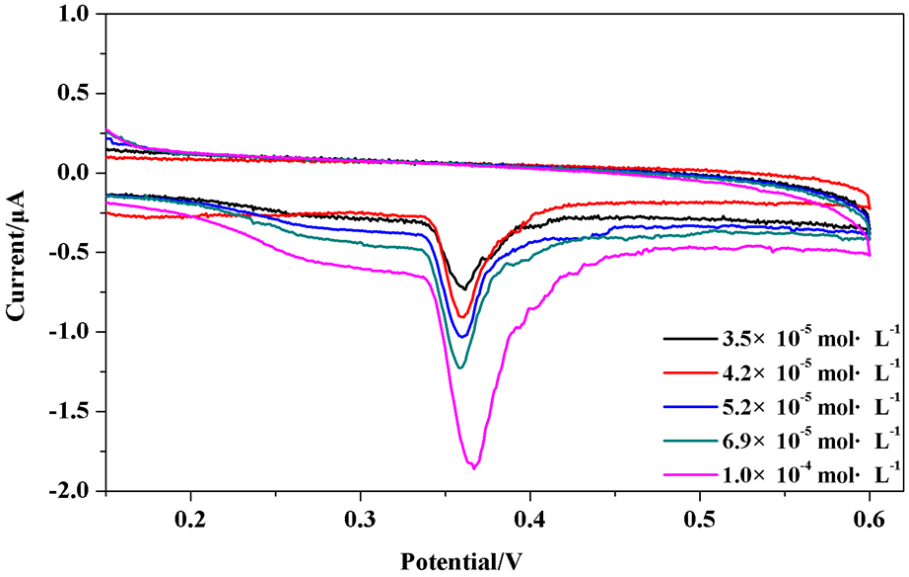

Figure 6. Cyclic voltammetric response of Fe_3O_4/Ag-GCE to methomyl at different concentrations ($V_{Fe_3O_4/Ag}$ =10μL, scanning rate=0.05 V/s, pH=6.9, T=298 K)

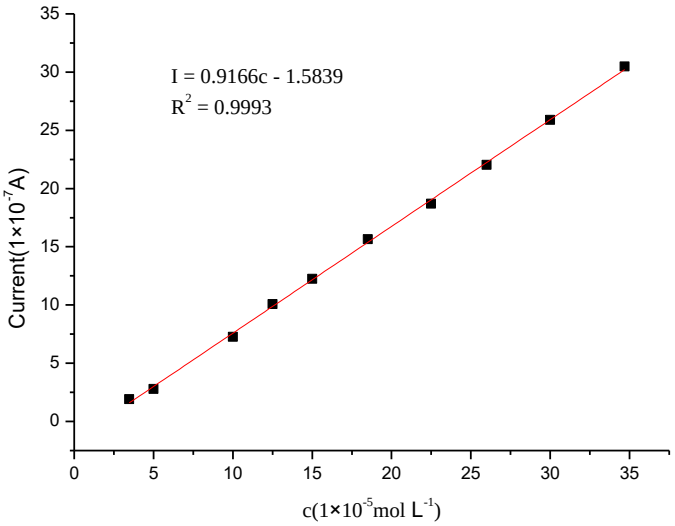

Figure 7 The current response of Fe_3O_4/Ag-GCE in methomyl at different concentrations ($V_{Fe_3O_4/Ag}$ =10μL, scanning rate=0.05 V/s, pH=6.9, T=298 K)

Under the optimized conditions, methomyl at different concentrations was investigated by cyclic voltammetry. The results in Fig. 6, no oxidation peak appeares in the lower half of the scanning curve, whereas an obvious reduction peak appeares in the upper half of the curve. Moreover, as the concentration of the methomyl increases, the reduction peak value gets more negative.

A good linear relationship between the reduction peak current and concentration of methomyl was established in the concentration range of 3.47×10^{-5}～3.47×10^{-4} mol·L^{-1}. The linear regression equation and linear coefficient are shown in Fig. 7.

3.5 Discussion on the mechanism

Using a gold electrode in a neutral electrolyte, Mijin et al. quantitatively measured methomyl via cyclic linear sweep voltammetry[16], wherein the quantitative determination was achieved in the concentration range of 4.0-16 mg L^{-1}. The reduction peak observed in the previous section indicates the reduction threshold of methomyl corresponding to the irreversible 4e reduction[17,18]. Other kind electrochemical sensors have been developed taking advantage of nanomaterials. Carbon nanotubes with core-shell structure were used to modify the glassy carbon electrode, and the sensitivity in the measurement of methomyl was greatly enhanced[19]. It is then hypothesized the excellent performance of the electrode upon modification with nanomaterial is mainly due to the high electrical conductivity and large surface area offered by the coated nanocomposites, and potential binding between nanocomposites and the analytes. All the aforementioned factors promote electron-transfer reactions.

3.6 Applications

Based on the results described above, we carried out a detailed analysis for potential applications. First, the edible parts of lettuce, rape, and spinach samples were torn to shreds. Then, 10.00 g of the shreds was put into a beaker, 50 mL of phosphate buffer was added and followed by sonication for 5

mins. We then brought the mixture to room temperature and collected the liquid through filtration. We transferred 1.0 mL, 2.5 mL, 5.0 mL and 50 mL of the liquid phase of the lettuce, rape, and spinach samples, respectively, into a volumetric flask in turn. Under the optimized experimental conditions, we added phosphate buffer to the scale. Finally, we added the standard solution of methomyl and conducted 3 parallel tests, took the average value, and calculated the recovery rate using the following formula:

Recovery rate = [(standard sample test value- sample test value) / (the added standard amount)] × 100%}.

The comparison of the results determined with the Fe_3O_4/Ag-GCE sensor and those with LC-MS/MS [20] are shown in Table 1. The results determined with the Fe_3O_4/Ag-GCE sensor are consistent with the standard method. Standard methods for the detection of carbamate pesticides are expensive and time-consuming. Thus, electroanalytical methods are considered to be rapid, simple and low-cost alternatives. It can be concluded that methomyl can be completely recovered by the present method, and therefore, the present method is suitable for residual quantity detection of methomyl.

Table 1 Sample determinations（n=3）

vegetable samples	Results of sample determined with Fe_3O_4/Ag-GCE sensor（$mg \cdot kg^{-1}$）	Results of sample determined by standard method（$mg \cdot kg^{-1}$）	Relative error（%）	Recovery rate（%）	RSD（%）
lettuce	0.0215	0.0213	1.0	96.45%	1.3
oilseed rape	0.0325	0.0328	-0.91	93.08%	2.1
spinach	0.0121	0.0119	1.7	94.42%	1.7

The reported methods[21-29] for detection of pesticides possess high selectivity, adequate sensitivity and reliability. However, they are usually time-consuming, costly, and have to be performed by skilled manpower and rely upon sophisticated instruments, making these approaches not suitable for regular food safety monitoring. The electrochemical Sensor modified with Fe_3O_4/Ag showed satisfactory linear range, suitable stability, fast response time, and good repeatability and reproducibility. The biosensor is easy to operate and it satisfies the safety standard for maximum residue limits for pesticides in food (National food safety standard (China), GB2763-2012) [30].

4. CONCLUSIONS

In summary, we have successfully prepared Fe_3O_4/Ag nanocomposites with core-shell structures. The as-prepared nanocomposites were then used to modify the glassy carbon electrode (GCE) surface. Compared to the results of the standard method, the present method shows an impressive recovery rate. It was concluded that the electrochemical sensor prepared in the present work possesses certain advantages such as easy to operate, low cost, stable, accurate and fast, that are superior to previously reported electrochemical sensors. Along with its lower detection limit and wider linear range, the as prepared sensor becomes a good candidate for an alternative enzymatic biosensors, specifically in the

detection of methomyl in vegetables.

ACKNOWLEDGEMENTS

This research was financially supported by Gansu Provincial Sci & Tech Department SME Innovation Fund (1604JCCM126).

References

1. W. Jin, C. Li, L. Qian, *Chin. J. Health Lab. Tech.*,23(2013)1082.
2. C. Sun, H. Bi, H. Zhang, Y. Rao, M. Ma, *Ecol. Environ.*, 3(2007)887.
3. W. J. Li, *J. Jilin Univ.*, 2017.
4. Y. Ni, T. Zhu, Q. Yan, *Test. Chem. Anal.(Part B: Chem. Anal.)*, 53(2017)865.
5. Y. Cai, *Taiwan Agric. Res.*, 4(2012)70.
6. X. Wang, M. Zeng, D. Wan, H. Tang, B. Zhao, Y. Zhou, X. Liu, *J. Food Saf. Qual.*, 5(2014)4163.
7. J. Qi, R. He, Y. Zhang, L. Xu, *Food Res. Dev.* , 7(2007)109.
8. J. Liu, W. Liu, Y. Teng, M. Lan, S. Ma, R. Yuan, J. Nie, C. He, *Spectrosc. Spec. Anal.*,37(2017)2061.
9. P. Luo, *Chem. Teac.*,2(2016)60.
10. H. Qu, Y. Li,X. Xie, Z. Wei,Y. Jin, *Acta Chim.. Sinica.*, 20(2007)2303.
11. E. Dumitrescu, S. Andreescu, *Methods Enzymol*, 589(2017)301.
12. R. Lin. T. Lim. T. Tran, *Electrochem. Commun.*, 86(2018)135.
13. W. Wu, J. Zhou, Y. Fang, Y. Liu, H. Gu, *Chem.*, 79(2016)1041.
14. H. Wei, J. Sun, Y. Wang, X. Li, G. Chen, Analyst,11 (2008) 1619.
15. A. J. Bard, L. R. Faulkner, Electrochemical Methods: Fundamental and Applications, John Wiley & Sons, (2001) Hoboken, U.S.A.
16. J. Serb, *Chem. Soc*., 74(2009)573.
17. M. Subbalakshmamma, M. Sreedhar, N. V. Jyothi, J. Damodar, S. J. Reddy, *Trans. SAEST,* 34(1999) 35
18. A. Ngoviwatchai, D. C. Johnson, *Anal. Chim. Acta,* 215(1988) 1
19. I. Cesarino, F. C. Moraes, M. R. V. Lanza, A. A. S. Machado, *Food Chemistry,* 135(2012) 873.
20. State Import and Export Commodities Inspection Bureau of the People's Republic of China. SN/T 0134-2010.
21. P. Wang, L. Wu, Z.C. Lu, Q. Li, W.M. Yin, F. Ding, H.Y. Han, *Anal. Chem.*, 89 (2017) 2424.
22. S.A. Nsibande, P.B.C. Forbes, *Anal. Chim. Acta*, 945 (2016) 9.
23. T. Tsuchiyama, M. Katsuhara, M. Nakajima, *J.Chromatogr.* A, 1524 (2017) 233.
24. M. Montemurro, L. Pinto, G. Véras, A.A. Gomes, M.J. Culzoni, M.C.U. Araújo, H.C. Goicoechea, *Talanta* 154 (2016) 208.
25. M. Liang, K. Fan, Y. Pan, H. Jiang, F. Wang, D. Yang, D. Lu, J. Feng, J. Zhao, L. Yang, X. Yan, *Anal. Chem*., 85 (2013) 308.
26. G. Fu, W. Chen, X. Yue, X. Jiang, *Talanta*, 103(2013) 110.
27. J. Gong, Z. Guan, D. Song, *Biosens. Bioelectron.*, 39 (2013) 320.
28. F. Yan, Y. He, L. Ding, B. Su, *Anal. Chem.*, 87 (2015) 4436.
29. N. Qiao, S. Qian, Y. Wang, H. Lin, *Talanta*, 181 (2018) 305.
30. National food safety standard (China), maximum residue limits for pesticides in Food (GB 2763-2012).